Available online at www.derpharmachemica.com

ISSN 0975-413X
CODEN (USA): PCHHAX

Der Pharma Chemica, 2016, 8(18):446-454
(http://derpharmachemica.com/archive.html)

Voltammetric study of Cu-Zn-Sn deposit

B. El Bahi, S. Cherrouf and M. Cherkaoui

Laboratory of Materials, Electrochemistry and Environment, Faculty of Sciences, Ibn Tofail University, Kenitra, Morocco

---

ABSTRACT

The electrodeposition of Cu-Sn-Zn coating on Cu substrate at ambient temperature was investigated. The bath consists of metal salts $CuSO_4$,$5H_2O$, $SnSO_4$, $ZnSO_4$,$7H_2O$ and sodium citrate ($NaC_6H_5Na_3O_7$,$2H_2O$) as complexing agent. To prevent precipitation, we varied the pH between 4 and 5.5. The voltammetric curves show four waves clearly defined corresponding to copper, tin and zinc reducing through $Cu_2HCit_2^{3-}$, $Sncit^{2-}$ and $ZnHcit^{-}$ complex respectively, the fourth peak being the reduction of protons. The influence of the concentration of the various bath constituents and the potential scan rate on the voltammetric curves was studied. We have shown that the deposition process of copper and tin is controlled by species mass transfer. For zinc deposition, the mechanism would be controlled by a mixed process: charge transfer and mass transport.

Keywords: Copper, tin, zinc, Cu-Sn-Zn, coating, citrate, electrodeposition, voltammetry.

INTRODUCTION

The thin-film solar cells have attracted the attention of numerous researchers the last ten years. Initially, the devices based $CuIn(Ga)Se_2$ (CIGS) had experienced significant growth due to their high conversion efficiency (21%) [1-2]. However, their development has been hampered by the toxicity and the rarity of certain elements, mainly indium and gallium [3-4].

Thus, kesterite structural alternatives, $Cu_2ZnSn(S_xSe_{1-x})_4$, have been proposed: Cu_2ZnSnS_4 (CZTS) [4-16], $Cu_2ZnSnSe_4$ (CZTSe) [3,17-21] and $Cu_2ZnSn(S,Se)_4$,(CZTSSe) [22-27]. These devices have high optical absorption coefficient (10^4 cm^{-1}) and bandgap ranging from 0.9 eV to 1.5 eV, very interesting for photovoltaic applications.

Synthesis of CZTSe(S) layers includes two steps: the formation of metallic precursor and the subsequent annealing under Se or S atmosphere at temperatures from 450 to 600 °C. Different methods have been used to develop the metal precursor CZT: Spin-coating [11, 27], co-sputtering [25], electrodeposition [21, 26, 29-30], pulse laser deposition [28], thermal evaporation [31-32], electroless plating [33], sol–gel method [34] and combustion [4]. The combustion method, based on the theory of propellant, is an extremely powerful tool to obtain metallic composite using corresponding metal salts–fuel mixtures. In some cases, it has been necessary to use a combination of two methods: Galvanostatic deposition to fabricate a composition-spread film of binary Sn–Zn alloys and a second step involving a water gun and weak copper sulfate solution used to achieve a composition spread film of ternary Cu–Sn–Zn alloys [35].

In developing the film CTZ, we opted for the electrochemical process which we thought was the least expensive, easiest to implement and most environmentally friendly. We noted that very few studies have examined the reduction mechanism of Cu-Zn-Sn alloy [26]. The main of this work is to conduct a voltammetric study of the Cu-Zn-Sn alloy deposition.

MATERIALS AND METHODS

The electrolysis cell is a borrosilcate glass (Pyrex®) cylinder closed by cap with five apertures. Three of them were used for the electrodes. The other two allow deaeration of the solution by bubbling nitrogen and temperature control. We used a copper with surface area of $1cm^2$ as working electrode, Pt plate as the counter electrode while SCE_{sat} as the reference electrode to which all potentials will be referred in the following. Prior to immersion test, the substrate was abraded using emery paper up to 2000 grade, cleaned with ethanol, etched in 10 % dilute sulfuric acid, washed with distilled water and dried finally. The baths contained copper sulfate ($CuSO_4$, $5H_2O$), tin sulfate ($SnSO_4$), zinc sulfate ($ZnSO_4$, $7H_2O$) and trisodium citrate ($NaC_6H_5Na_3O_7$, $2H_2O$) as complexing agent. The temperature was kept at 25 ± 1°C. The electrochemical measurements were carried out using Potentiostat/Galvanostat/Voltalab PGZ 100 monitored by a personal computer. The voltammetric measurements were performed in the potential range between 0.6 V to -1.8 V with different scan rate.

RESULTS AND DISCUSSION

Electrolyte stability

In order to achieve alloy deposits Cu-Zn-Sn by electrodeposition, it is imperative to add complexing agents in the metal salts bath. Different complexing agents were used: Citrate [10, 12, 26], tartaric acid [26], pyrophosphate [36]. In this study, we opted for citrate agent because citrate ions form various electroactive aqueous complexes with Cu (II), Sn (II) and Zn (II) [26]. The basic bath concentrations of tin sulfate, zinc sulfate and citrate were deduced from previous work on the Sn-Zn alloy electrodeposition [37]. The concentration of copper sulfate and pH were fixed relative to the thermodynamic model built by M. Slupska and P. Ozga [38]. The baths composition is given in table 1, the solutions were clear and no precipitates were observed. Figure 1 presents the diagram of phases and dominant species of copper, tin and zinc depending on the sodium citrate concentration and the relationship between the potential and pH [38].

Table1: Baths composition

Electrolytes	$CuSO_4$, $5H_2O$ (mol/L)	$SnSO_4$ (mol/L)	$ZnSO_4$, $7H_2O$ (mol/L)	$NaC_6H_5Na_3O_7$, $2H_2O$ (mol/L)	pH
1	-	-	-	0.4	4
2	0.16	0.14	0.22	0.4	4
3	0.16	0.14	0.22	0.5	4
4	0.16	0.14	0.22	0.6	4
5	0.16	0.14	0.22	0.4	5
6	0.16	0.14	0.22	0.4	5.5
7	0.20	0.14	0.22	0.4	4
8	0.24	0.14	0.22	0.4	4
9	0.16	0.22	0.22	0.4	4
10	0.16	0.26	0.22	0.4	4
11	0.16	0.14	0.30	0.4	4
12	0.16	0.14	0.34	0.4	4

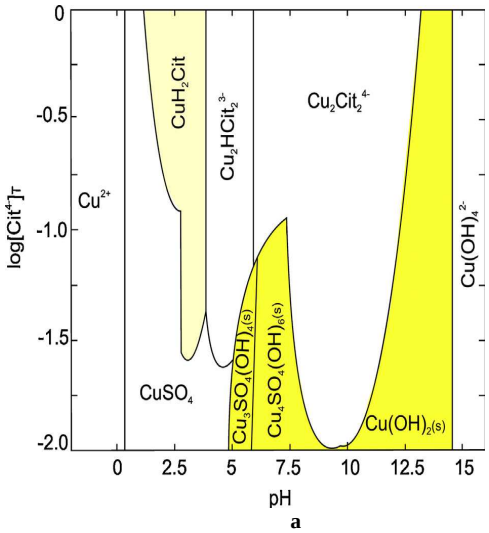

a

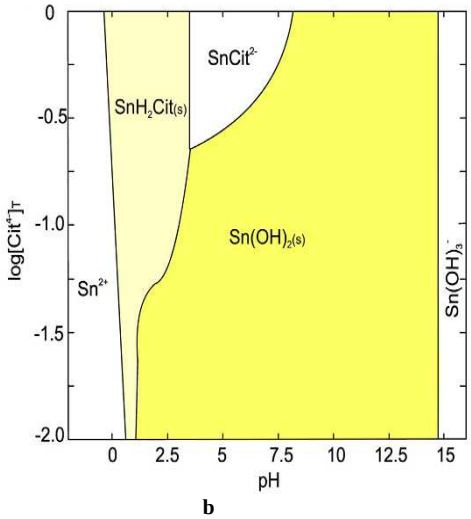

b

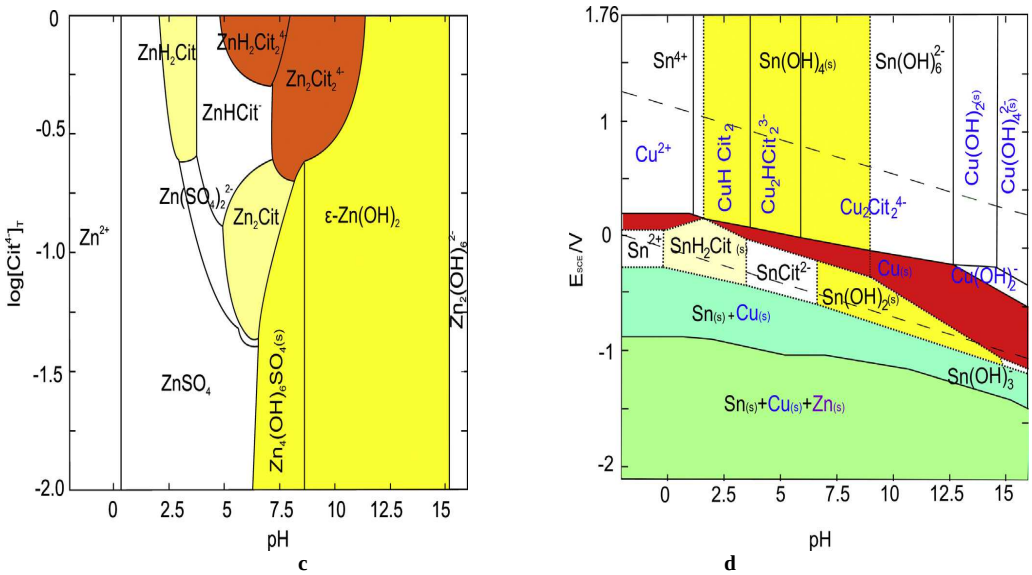

Figure 1: Predominance area diagram : a- for Cu(II) species, b- for Sn(II) species, c- for Zn(II) species, d- Potential (E)-pH diagram [38]

Voltammetric study

Sodium citrate concentration effect

Fig. 2 shows the voltammogram realized in the electrolyte (1) containing only sodium citrate at pH = 4. The increase in the cathodic current density from − 0.8 V is linked to protonated form of citrate ion according to reaction:

$$2H_3cit^{-} + 2\,e^{-} \longrightarrow H_2 + 2H_2cit^{2-} \qquad (1)$$

Then, a sharp increase occurs at -1.15 V due to the hydrogen evolution.

$$2H^{+} + 2\,e^{-} \longrightarrow H_2 \qquad (2)$$

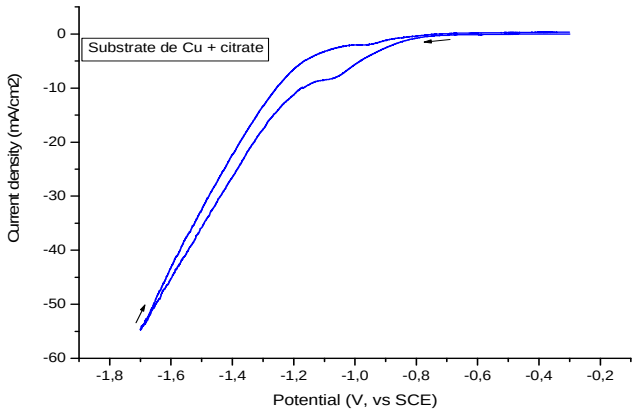

Figure.2: Cyclic voltamogramm on a Cu substrat in citrate solution at pH = 4 (electrolyte 1), scan rate v = 25 mV/s

After addition of metal salts (electrolyte 2) to the sodium citrate solution, we observe in cathodic area four waves clearly defined as has been reported by various authors [26, 38] (fig.3). The first wave with peak at –0.30 V (a_1) corresponds to Cu (II) reduction. Then, tin deposition starts around -0.70 V, the wave reaches the maximum at –0.88 V (b_1). The third wave (c_1) is attributed to hydrogen evolution (-1.1 V) and the fourth one (d_1) to zinc deposition (-1.5V). The deposition processes for tin, zinc and copper is in accordance with the order of their equilibrium reduction potentials (Cu(II)/Cu, Sn(II)/Sn, Zn(II)/Zn; therefore, this type of co-deposition is normal, according to the Brenner classifications [39]. During the reverse scan, three peaks appeared corresponding to zinc (d_2), tin (b_2) and copper (a_2) oxidation (fig.3).

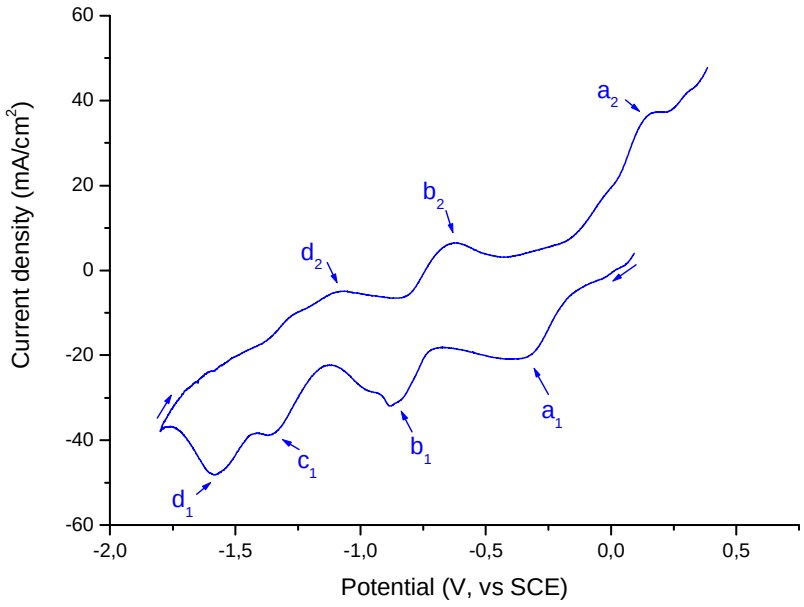

Figure 3: Cyclic voltamogramm on a Cu substrat in 0.16 mol/L $CuSO_4$, 0.14 mol/L $SnSO_4$, 0.22 mol/L $ZnSO_4$ and 0.4 mol/L citrate at pH = 4 (electrolyte 2), scan rate v = 25 mV/s

An increase in the concentration of citrate (electrolyte 2-4) induces, as expected, a displacement of Cu (II), Sn (II) and Zn (II) reduction potentials towards more cathodic values, the stannous ion being most sensitive to this complexing agent (fig.4).

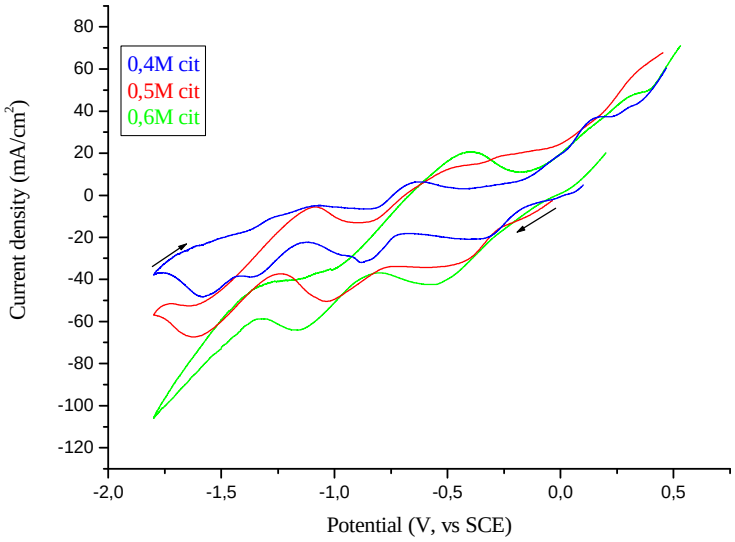

Figure 4: Cyclic voltamogramm on a Cu substrat in 0.16 mol/L $CuSO_4$, 0.14 mol/L $SnSO_4$, 0.22 mol/L $ZnSO_4$ and 0.4; 0.5 and 0.6 mol/L citrate at pH = 4 (electrolyte 2-4), scan rate v = 25 mV/s.

Indeed, the complexation of a metallic ion by a ligand, L, occurs according to

$$M^{n+} + a\ L^{b} \underset{2}{\overset{1}{\rightleftharpoons}} (ML_a)^{n+ab} \qquad (3)$$

With the complexation constant:

$$K_c = [(ML_a)^{n+ab}] / [M^{n+}][L^{b}]^{a} \qquad (4)$$

The deposition of the metal M occurs according to:

$(ML_a)^{n+ab} + ne^- \rightleftharpoons M + a\,L^b$ (5)

With an equilibrium potential given by Nernst equation:

$E = E^\circ + (RT/nF)\,Ln\,[(ML_a)^{n+ab}] / [L^b]^a\,(M) = E^\circ + (RT/nF)\,Ln\,K_c\,[M^{n+}]$ (6)

where E° is the standard potential of the $(ML_a)^{n+ab}/M$ couple, n the number of exchanged electrons in the deposition reaction, F the Faraday's constant (96487 C mol^{-1}), T the temperature (Kelvin), R the molar gas constant (8.31 J. mol^{-1}. K^{-1}) and $[M^{n+}]$ metal ion concentration, $[L^b]$ ligand concentration, $[(ML_a)^{n+ab}]$ complex concentration and (M) metal activity (= 1 by convention).

When the ligand concentration increases (citrate), the equilibrium (3) is moved in the direction 1 leading to a higher consumption of the metal ion and consequently a reduction of its concentration. So the equilibrium potential, according to the equation (6) will decrease. Furthermore, we noticed an increase in the cathodic current density with the citrate concentration due to greater stability of the bath.

pH effect

When the pH is adjusted to 3, we see instability of the bath over the long term. By cons, when the pH increase (4 to 5.5), the bath still stable. The shape of the I-V curves is practically unchanged however we are seeing a decrease in the reduction current and a shift of peak potentials to slightly more cathodic values (Fig. 5). In fact, the predominant forms of metal-citrate complexes are $Cu_2HCit_2^{3-}$, $Sncit^{2-}$, $ZnHcit^-$ [38] so the reactions occurring would be:

$Cu_2HCit_2^{3-} + 5H^+ + 4e^- \leftrightarrow 2Cu + 2H_3Cit^-$ 7

$Sncit^{2-} + 3H^+ + 2e^- \leftrightarrow Sn + H_3cit^-$ 8

$ZnHcit^- + 2H^+ + 2e^- \leftrightarrow Zn + H_3cit^-$ 9

With equilibriums potentials

$E_6 = E_6^\circ + (RT/nF)\,Ln\,([Cu_2HCit_2^{3-}]\,[H^+]^5 / [H_3Cit^-]^2)$

$= E_6^\circ - 0.075\,pH + 0.015\,log\,([Cu_2HCit_2^{3-}] / [H_3Cit^-]^2)$ 10

$E_7 = E_7^\circ + (RT/nF)\,Ln\,([Sncit^{2-}]\,[H^+]^3 / [H_3Cit^-])$

$= E_7^\circ - 0.09\,pH + 0.03\,log\,([Sncit^{2-}] / [H_3Cit^-])$ 11

$E_8 = E_8^\circ + (RT/nF)\,Ln\,([ZnHcit^-]\,[H^+]^2 / [H_3Cit^-])$

$= E_8^\circ - 0.06\,pH + 0.06\,log\,([ZnHcit^-] / [H_3Cit^-])$ 12

E°: Standard potential of (metal-citrate complexes /metal) couple, n: number of exchanged electrons, F = 96487 C mol^{-1}, T = 298°K, R = 8.31 J. mol^{-1}. K^{-1}, Ln = 2.3 log

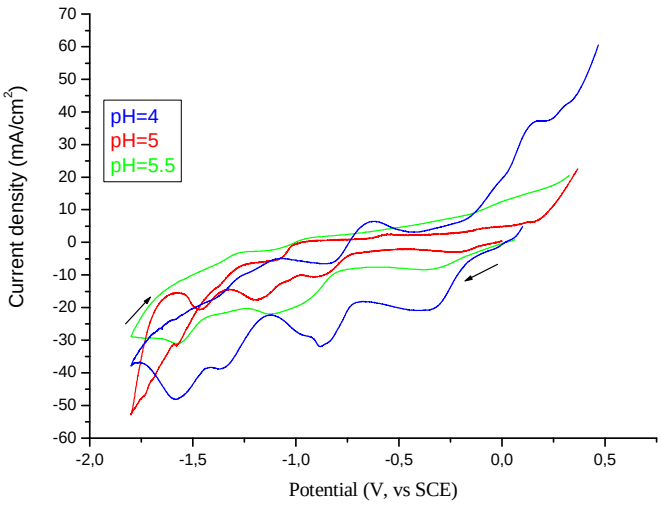

Figure 5: Cyclic voltamogramm on a Cu substrat in 0.16 mol/L $CuSO_4$, 0.14 mol/L $SnSO_4$, 0.22 mol/L $ZnSO_4$ and 0.4mol/L citrate at pH 4 to pH 5.5 (electrolytes 2; 5-6), scan rate v = 25 mV/s

An increase in pH and therefore the decrease of proton (H^+) concentration causes the equilibriums (6, 7 and 8) displacement to the left thus inhibits the deposition. This involves a decrease of the cathodic current. Relations 10-12 confirm that pH elevation shifts the peak potentials towards more cathodic values.

Effect of the metal salts concentration

Figures 6 and 7 show the voltammograms carried out at different concentrations of copper sulphate and tin sulfate (electrolytes 2, 7-10). As expected, Cu (II) and Sn (II) peaks reduction increase respectively with $CuSO_4$ and $SnSO_4$ concentrations. By against, the increase of $ZnSO_4$ concentration (electrolytes 2, 11-12) induced elevation of the three reduction peaks (fig. 8). These observations indicate that no interaction occurs during the CZT deposition between copper and tin.

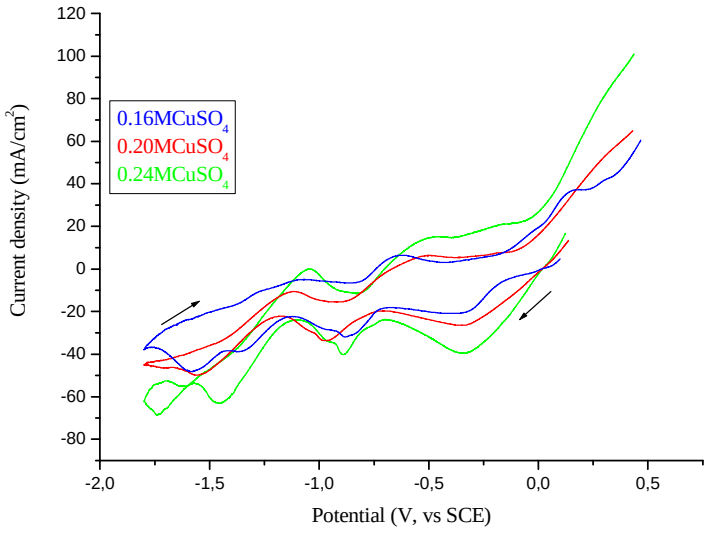

Figure 6: Cyclic voltamogramm on a Cu substrate in 0.16 mol/L, 0.20 Mol/L and 0.24 mol/L $CuSO_4$, 0.14 mol/L $SnSO_4$, 0.22 mol/L $ZnSO_4$,0.4mol/L citrate at pH = 4 ,(electrolytes 2; 7-8), scan rate v = 25 mV/s

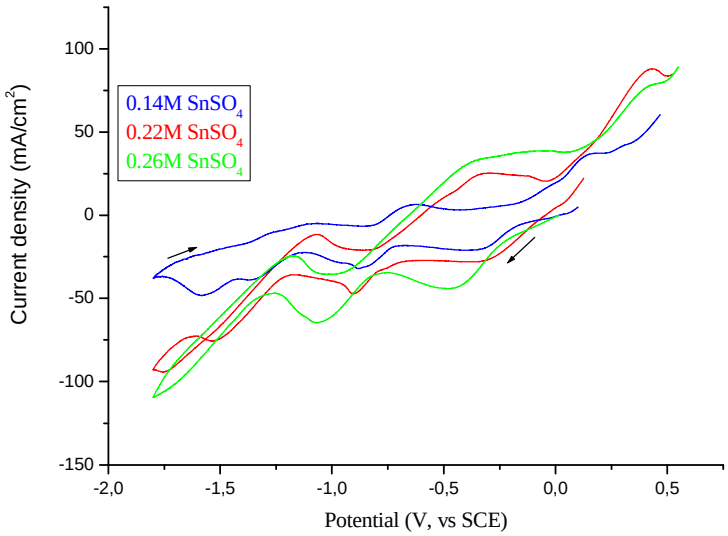

Figure 7: Cyclic voltamogramm on a Cu substrate in 0.16 mol/L $CuSO_4$, 0.14 mol/L, 0.22 Mol/L and 0.26 mol/L $SnSO_4$, 0.22 mol/L $ZnSO_4$, 0.4mol/L citrate at pH = 4 (electrolytes 2; 9-10), scan rate v = 25 mV/s

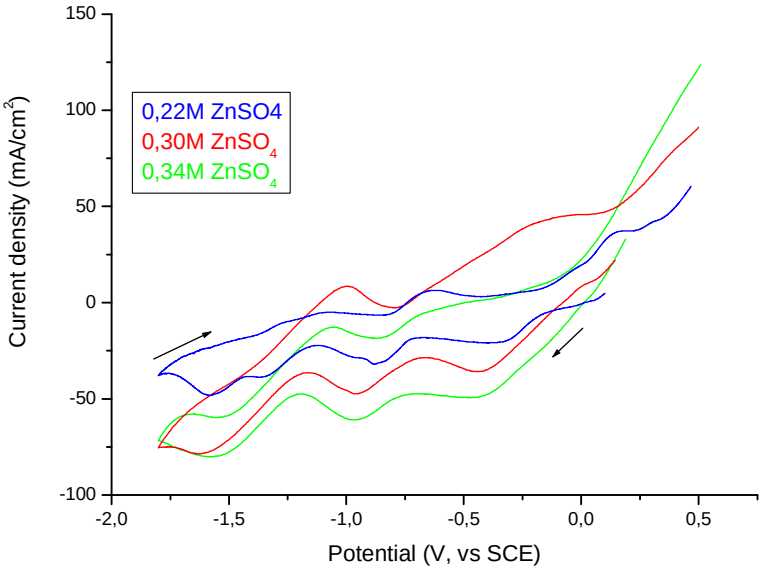

Figure 8: Cyclic voltamogramm on a Cu substrate in 0.16 mol/L $CuSO_4$, 0.14 mol/L $SnSO_4$, 0.22 mol/L, 0.30mol/L and 0.34 mol/L $ZnSO_4$, 0.4mol/L citrate at pH = 4 (electrolytes 2; 11-12), scan rate v = 25 mV

Influence of the potential scanning rate

Figure 9 shows the voltammograms carried out at various potentials scanning rate. All reduction waves increase with the potential scan speed. Cu(II) and Sn (II) reduction peaks vary linearly according to the square root of the potential scan rate with an intercept close zero indicating a deposition process of the two metals controlled by species mass transfer (fig. 10a and 10b) [37].

Indeed, in the case of a linear and semi-infinite diffusion, the peak current Ip is equal to [40]:

$$Ip\ (A) = 2.69.10^5\ n^{3/2}\ A\ D^{1/2}\ v^{1/2}\ C \qquad 13$$

n: electron exchanged, A : electrode area (cm^2), D : Diffusion coefficient ($cm^2.s^{-1}$), v: potential scan rate ($V.s^{-1}$) C : Specie concentration ($mol.cm^{-3}$)

For the zinc deposition, the peak is not proportional to $v^{1/2}$. The mechanism would be controlled by a mixed process: charge transfer and mass transport [26].

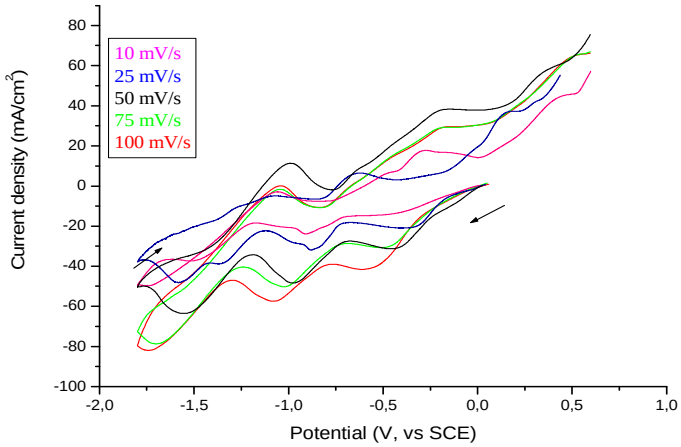

Figure 9: Cyclic voltamogramm on a Cu substrat in 0.16 mol/L $CuSO_4$, 0.14 mol/L $SnSO_4$, 0.22 mol/L $ZnSO_4$, 0.4mol/L citrate at pH = 4 (electrolytes 2), scan rate v = 10 to 100 mV/s

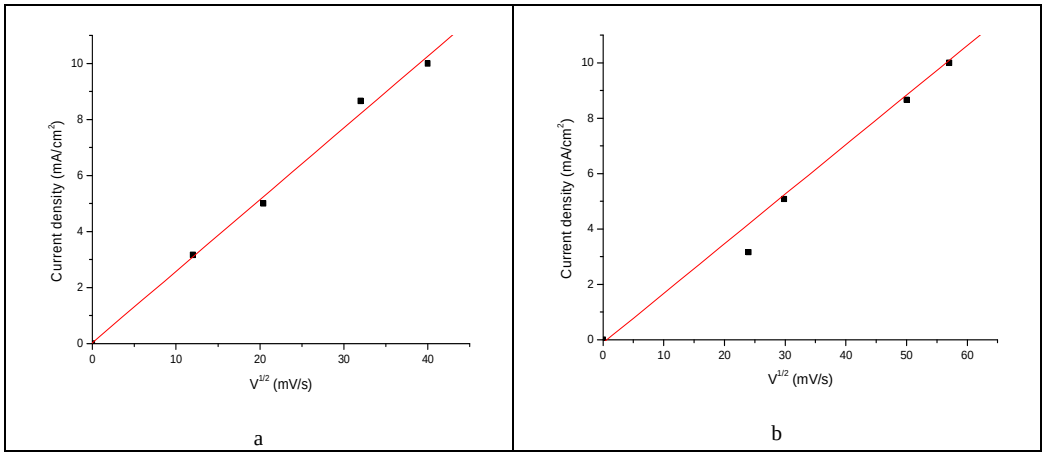

Figure 10: Peak current density as a function of the square root of scanning speed potential (electrolyte 2), a- Copper peak, b- Tin peak

CONCLUSION

The voltammetric study of the alloy Cu-Zn-Sn deposit showed that the deposition process of tin, zinc and copper is the normal type in accordance with the order of their reduction potentials. At pH=5, Cu(II), tin(II) and zinc(II) were reduced via complex Cu-citrate ($Cu_2HCit_2^{3-}$), Sn-citrate ($Sncit^{2-}$) and Zn-citrate ($ZnHcit^{-}$) respectively. An increase in the concentration of citrate and the pH shift the peak potentials towards more cathodic values. Cu(II) and Sn(II) reduction peaks vary linearly according to the square root of the potential scan rate with an intercept close zero indicating a deposition process controlled by species mass transfer. For zinc, deposition would be controlled by a mixed process: charge transfer and mass transport

REFERENCES

[1] M. Repnis, M. Contreras, B. Egaas, C. Dehart, J. Scharf, C. Perkins, B. To, R .Noufi, *Prog. Photovol.*, **2008**, 16, 235–239
[2] A. Chirila, S. Buecheler, F. Pianezzi, P. Bloesch, C. Gretener, A.R. Ulh, C. Fella,L. Kranz, J. Perrenound, S. Seyrling, R. Verma, S. Nishiwaki, Y.E. Romanyuk, G.Bilger, A.N. Tiwari, *Nat. Mater*., **2011**, 10, 857–861.
[3] Zhesheng Chena, Lei Hanb, Lei Wanb, Chunhui Zhanga, Haihong Niua, Jinzhang Xu, *Appl. Surf. Sci*., **2011**, 257, 8490–8492.
[4] Xin Jin, Jianmin Li, Guilin Chen, Cong Xue, Weifeng Liu, Changfei Zhu, *Solar Energy Materials & Solar Cells*, **2016**, 146, 16–24.
[5] H. Katagiri, *Thin Solid Films*, **2005**, 426, 480–481.
[6] H. Araki, A. Mikaduki, Y. Kubo, T. Sato, K. Jimbo, W.S. Maw, H. Katagiri, M.Yamazaki, K. Oishi, A. Takeuchi, *Thin Solid Films*, **2008**, 517, 1457-1460.
[7] H. Katagiri, K. Jimbo, W.S. Maw, K. Oishi, M. Yamazaki, H. Araki, A. Takeuchi, *Thin Solid Films*, **2009**, 517, 2455–2460.
[8] H. Araki, Y. Kubo, K. Jimbo, W.S. Maw, H. Katagiri, M. Yamazaki, K. Oishi, A. Takeuchi, *Phys. Status Solidi* C, **2009**, 6,1266–1268.
[9] R. Schurr, A. Holzing, S. Cost, R. Hock, T. Vob, J. Schulze, A. Kirbs, A. Ennaoui, M. Lux-Steiner, A. Weber, I. Kotschau, H.W. Schock, *Thin Solid Films*, **2009**, 517 2465–2468.
[10] S.M. Pawar, B.S. Pawar, A.V. Moholkar, D.S. Choi, J.H. Yun, J.H. Moon, *Electrochim. Acta*, **2010**, 55, 4057-4061.
[11] T. Tanaka, A. Yoshida, D. Saiki, K. Saito, Q. Guo, M. Nishio, T. Yamaguchi, *Thin Solid Films*, **2010**, 518, S29-33.
[12] B.S. Pawar, S.M. Pawar, S.W. Shin, D.S. Choi, C.J. Park, S.S. Kolekar, J.H. Kim, *Appl. Surf. Sci*., **2010**, 257, 1786-1791.
[13] K. Tanaka, Y. Fukui, N. Moritake, H. Uchiki, *Sol. Energy Mater. Sol. Cells*, **2011**, 95, 838-842.
[14] T. Washio, H. Nozaki, T. Fukano, T. Motohiro, K. Jimbo, H. Katagiri, *J. Appl. Phys*. **2011**, 110 (074511), 1–4.
[15] J. He, L. Sun, K. Zhang, W. Wang, J. Jiang, Y. Chen, P. Yang, J. Chu, *Appl. Surf. Sci.*, **2013**, 264, 133–138.
[16] M.I. Amal, K.H. Kim, *Thin Solid Films*, **2013,** 534, 144–148.
[17] G. Suresh Babu, Y.B. Kishore Kumar, P. Uday Bhaskar, V. Sundara Raja, *Sol Energy Mater Sol. Cells*, **2010**, 94, 221-226

[18] Z. Chen, L. Han, L. Wan, C. Zhang, H. Niu, J. Xu, *Appl. Surf. Sci.* **2011,** 257, 8490–8492.
[19] R. Juskenas, S. Kanapeckaite, V. Karpaviciene, Z. Mockus, V. Pakstas, A. Selskiene, R. Giraitis, G. Niaura, *Sol. Energy Mater. Sol. Cells*, **2012**, 101, 277-282.
[20] T. Maeda, S. Nakamura, T. Wada, *Thin Solid Films*, **2011**, 519, 7513-7516.
[21] R. Kondrotas, R. Juškėnas, A. Naujokaitis, G. Niaura, Z. Mockus, S. Kanapeckaitė, B. Čechavičius, K. Juškevičius , E. Saucedo, Y. Sánchez, *Thin Solid Films*, **2015**, 589, 165–172
[22] O. Gunawan, T. Gokmen, C.W. Warren, J.D. Cohen, T.K. Todorov, D.A.R. Barkhouse, S. Bag, J. Tang, S. Byungha, D.B. Mitzi, *Appl. Phys. Lett*., **2012**, 100, 253905.
[23] T.K. Todorov, J. Tang, S. Bag, O. Gunawan, T. Gokmen, Y. Zhu and D. Mitzi, *Adv. Energy Mater*., **2011**, 3 (1) 34-38.
[24] S.M. Lee, Y.S. Cho, *J. Alloys Comp*. **2013**, 579, 279–283.
[25] A. Fairbrother, X. Fontané, V. Izquierdo-Roca, M. Espíndola-Rodríguez, S. López-Marino, M. Placidi, J. López -Garcia, A. Pérez-Rodríguez, E. Saucedo, *Chem Phys Chem*., **2013**, 14 (9) 1836-1841.
[26] C. Gougaud, D. Rai, S. Delbos, E. Chassaing, D. Lincot, *J. Electrochem. Soc*., **2013**, 160 (10) D 485-494.
[27] J. Kim, J. Hiroi, T.K. Todorov, O. Gunawan, M. Kuwahara, T. Gokmen, D. Nair, M. Hopstaken, B. Shin, Y.S. Lee, W. Wang, H. Sugimoto, D.B. Mitzi, *Adv. Mater*., **2014**, 26 (44) 7427-7431.
[28] K. Moriya, K. Tanaka, H. Uchiki, *Jpn. J. Appl. Phys*., **2007**, 46, 5780-5781.
[29] F. Jiang, S. Ikeda, T. Harada, M. Matsumura, Adv. Energy Mater. **2014**, 4, 7-11.
[30] J. Li, T. Ma, M. Wei, W. Liu, G. Jiang, C. Zhu, *Appl. Surf. Sci*. **2012**, 258, 6261-6265.
[31] L. Shao, J. Zhang, C. Zou, W. Xie, *Phys. Proc*., **2012**, 32, 636-640.
[32] B. Shin, O. Gunawan, Y. Zhu, N.A. Bojarczuk, S.J. Chey, S. Guha, *Prog. Photovolt. Res. Appl*. **2013**, 21, 72–76.
[33] Xe Xin-kuai, Chen Bai-zhen, Hu Geng-sheng, Deng Ling-feng, Zhou Ning-bo, Tian Wen-zeng, *Trans.Nonferrous Met. Soc. China*, **2006**, 16, 223-228.
[34] K. Tanaka, N. Moritake, H. Uchiki, *Sol. Energy Mater. Sol. Cells*, **2007**, 91, 1199–1201.
[35] S.D. Beattiea, J.R. Dahn, *J. of Electrochem. Soc*. **2005**, 152, C 542-548.
[36] A. Ennaoui, M. Lux-Steiner, A. Weber, D. Abou-Ras, I. Kötschau, H. W. Schock, R. Schurr, A. Hölzing, S. Jost, R. Hock, T. Voß, J. Schulze, and A. Kirbs, *Thin Solid Films*, **2009**, 517, 2511-2514
[37] Y. Salhi, S. Cherrouf, M. Cherkaoui, K. Abdelouahdi, *Appl. Surf. Sci.*, **2016**, 367, 64–69.
[38] M. Slupska, P. Ozga, *Electrochim. Acta*, **2014**, 141, 149-160.
[39] A. Brenner, Electrodeposition of Alloys, Academic Press, New York, **1963**, vols.1 and 2
[40] A.J. Bard and L.R. Faulkner, Electrochimie, Principes, Méthodes et Applications, Edit. Masson, **1983**.